Use of the independent-particle model to treat curve-crossing transitions

L. F. Errea,[1] A. Macías,[1,2] L. Méndez,[1] and A. Riera[1]
[1]*Laboratorio Asociado al CIEMAT de Física Atómica y Molecular en Plasmas de Fusión, Departamento de Química C 9, Universidad Autónoma de Madrid, Cantoblanco E-28049 Madrid, Spain*
[2]*Instituto de Estructura de la Materia CSIC, Serrano 113 bis, 28006 Madrid, Spain*
(Received 23 February 2001; published 20 August 2001)

We discuss the usefulness of the independent-particle model to describe charge-transfer processes. We consider, as a benchmark case, avoided crossing transitions in two-electron systems, described by means of the Landau-Zener-Stueckelberg model. It is shown that the independent-particle model, with an equivalent-electron interpretation of the one-electron transition probabilities, reproduces single-electron transition probabilities for a wide range of physical situations. Significant deviations with respect to a two-electron calculation are related to Stueckelberg oscillations of the transition probabilities.

DOI: 10.1103/PhysRevA.64.032714 PACS number(s): 34.70.+e

I. INTRODUCTION

While theoretical methods to describe collisions in one-electron systems are well established (see, e.g., [1]), there are no specific methods for many-electron systems, whose description is usually based on the application of the independent-particle approximation, in which the many-electron problem is reduced to several one-electron problems. Although the use of the independent-particle approximation is standard in atomic and molecular structure calculations (see, e.g., [2]), where it is the basis of the widely employed Hartree-Fock method, there is no equivalent approach that can be systematically applied to dynamical problems, as the time-dependent Hartree Fock method is difficult to apply and not free from convergence problems (see [3] and references therein). On the other hand, the independent particle approximation has been applied to ion-atom collisions within different formalisms (see, e.g., Refs. [4,5] for the application in close coupling atomic and molecular treatments; Refs. [6,7] for CTMC calculations; and [8] for CDW calculations). It has been also applied in collisions of atoms with clusters [9], and, in connection with semiclassical models [10], to describe experimental results of single and double capture from atomic and molecular targets [11]. It should be noted, however, that the theoretical basis of the method is by no means obvious.

The simplest situation in which the approximation is applied involves systems with a clear distinction between an active electron and the remainder (core) electrons, such as in proton-alkaline collisions [12] or collisions of closed-shell multicharged ions–H collisions, e.g., C^{4+}-H (see [13]). The treatment of these collisions is often carried out by employing effective potentials to describe the interaction of the active electron with the atomic cores, and several model potentials and pseudopotentials have been proposed [14]. Furthermore, the use of effective potentials has been extended to systems with two active electrons outside a closed-shell core [15]. A different extension of the method involves the description by means of effective potentials of the H^- open-shell core (see [16] for H^+-H^- and [17] for He^{2+}-H^- collisions). The use of time-dependent model potentials has also been suggested (see Refs. [18,3]).

In the independent-particle approximation, the Hamiltonian of the system is expressed as the sum of one-electron effective Hamiltonians. The corresponding one-electron transition probabilities are then evaluated in a relatively simple way, and the final probabilities are obtained by using a many-electron interpretation. The most common interpretation [19] assumes that all electrons are equivalent. In this paper and following this usage we shall call the independent-particle model (IPM) the independent-particle approximation with the equivalent electron interpretation.

Alternative treatments in which core and active electrons are not equivalent have also been proposed [20,21], and this idea has been used in models and calculations of double capture [22,23] and double ionization [24] of He by ion impact. Equivalent and nonequivalent models thus coexist, and in many cases it is not obvious which, if any, is the most appropriate one to use [1]. This is mainly because few calculations [25–27] have compared equivalent and nonequivalent treatments. There are also situations in which the method is implicitly used: As will be explained in the following section, there is a limit of the nonequivalent treatment in which only the active electron undergoes transitions, so that it does not appear to require the use of any many-electron interpretation (see, e.g., Refs. [12,13,28,29]). Another alternative to the usual IPM has been recently proposed [30,31,3] for H^+ collisions with many-electron targets, which assumes that the transfer of one electron blocks further electron transfer, which in practice means that the single capture cross section is increased by adding to it the corresponding ones for *N*-electron capture.

In recent works [27,32], we have employed model potential techniques to evaluate charge-transfer cross sections in ion-H_2 collisions by using a model potential to describe the interaction of the active electron with the H_2^+ core. These works have pointed out that the two-electron interpretation of the one-electron probabilities is indispensable, and partially explained the success of the IPM at high velocities, while at low velocities, single-electron capture cross sections showed an important disagreement with *ab initio* results that was explained as a consequence of the incorrect transition probabilities for double electron capture in the IPM (see [1] and references therein, [4,33,7], and [34]).

The analyses of Refs. [27,32] were based on a comparison of Hamiltonian matrix elements, but the consequences in the dynamics of the differences in Hamiltonian matrices was not considered. The aim of the present paper is to carry out model calculations that yield insight into the properties of the independent electron approaches. For this purpose, we shall consider a two-electron system in which transitions leading to single-electron transfer take place at an avoided crossing of two potential-energy curves, and the Landau-Zener-Stueckelberg (LZS) model [35–37] will be used for the corresponding energies and couplings.

The paper is organized as follows. In Sec. II, we will introduce the basic equations for our comparison between ''exact'' and IPM model calculations; in it we will apply the conclusions of Refs. [27] and [32] to relate one- and two-electron Hamiltonian matrix elements. In Sec. III, we carry out the comparisons using the simple Landau-Zener model, and in Section IV we do so with the LZS model. Conclusions are drawn in Sec. V. Atomic units are used unless otherwise stated.

II. THEORY

A. Two-electron and single-electron approaches

We employ a semiclassical eikonal description of the collision, where the nuclei follow rectilinear nuclear trajectories, with impact parameter **b** and constant velocity **v**, $\mathbf{R}=\mathbf{b}+\mathbf{v}t$, and the electronic motion is described by means of the semiclassical eikonal equation. For a two-electron system, it has the form

$$\left(H-i\frac{\partial}{\partial t}\right)\Psi(\mathbf{r}_1,\mathbf{r}_2,t)=0, \tag{2.1}$$

where H is the nonrelativistic, fixed nuclei, electronic Hamiltonian. In the single-electron approaches, it is assumed that one (active) electron moves in the field created by the nuclei and the other the (core) electron. The interaction of the active electron with the core is represented by means of the effective potential included in the one-electron Hamiltonian, h. In this way, the electron-core interaction is taken into account in an average way by the effective potential, which is usually of the central type and static (see Ref. [14]), although in principle it could be taken to be time-dependent. The two-electron Hamiltonian H is then approximated by

$$H\simeq h(\mathbf{r}_1)+h(\mathbf{r}_2). \tag{2.2}$$

In the following, we shall assume that this approximation is sufficiently accurate for the present purposes. For instance, for the case of collisions between multicharged ions and H_2 molecules, the accuracy of approximation (2.2) was tested in Refs. [27,32] by explicit comparison of the Hamiltonian matrix elements of this equation with the corresponding *ab initio* ones.

In the equivalent electron treatment (called IPM in the present work), one uses $h=-1/2\nabla^2+V$ with V the effective potential. When the initial state is a singlet, the two-electron wave function Ψ is then written

$$\Psi(\mathbf{r}_1,\mathbf{r}_2,t)=||\psi\overline{\psi}||, \tag{2.3}$$

where ψ is a solution of the one-electron eikonal equation:

$$\left(h-i\frac{\partial}{\partial t}\right)\psi=0. \tag{2.4}$$

As mentioned in the Introduction, we consider a two-state problem. We expand the solutions of Eq. (2.4) in terms of two diabatic orbitals $\{\chi_1,\chi_2\}$, obtained by carrying out a unitary transformation on the basis of adiabatic molecular orbitals $\{\varphi_1,\varphi_2\}$ so that the radial components of the couplings $\langle\chi_i D|h-i(\partial/\partial t)|\chi_j D\rangle$ vanish, where D is a common translation factor (see Refs. [27,32]). The two-electron basis used to expand the solution of Eq. (2.1) is then chosen as antisymmetrized products of the diabatic spin orbitals $\chi_{1,2}$ $\overline{\chi_{1,2}}$. These functions are of the form

$$\phi^e_{ij}=\frac{N_{ij}}{\sqrt{2}}[||\chi_i\overline{\chi_j}||+||\chi_j\overline{\chi_i}||], \tag{2.5}$$

where $N_{ij}=1$ for $i\neq j$ and $N_{ij}=1/\sqrt{2}$ for $i=j$. Using Eq. (2.2), it is easily shown that one- and two-electron energy differences and (Hamiltonian) couplings are related through

$$\begin{aligned}&\langle\phi^e_{ij}|H|\phi^e_{ik}\rangle\simeq\sqrt{2}\langle\chi_j|h|\chi_k\rangle,\\ &\langle\phi^e_{ik}|H|\phi^e_{ik}\rangle-\langle\phi^e_{ij}|H^e|\phi^e_{ij}\rangle\simeq\langle\chi_k|h|\chi_k\rangle-\langle\chi_j|h|\chi_j\rangle.\end{aligned} \tag{2.6}$$

For comparison purposes, we also consider briefly the nonequivalent-electron treatment. We write in Eq. (2.2) $h=1/2(h^a+h^c)$, where different one-electron Hamiltonians h^c, h^a are used, respectively, for the core and active electrons. The two-electron wave function is now written as

$$\Psi(r_1,r_2)=\frac{1}{\sqrt{2}}[||\psi^c\overline{\psi^a}||+||\psi^a\overline{\psi^c}||], \tag{2.7}$$

where ψ^c, ψ^a are solutions of the equations

$$\left(h^c-i\frac{\partial}{\partial t}\right)\psi^c=0, \tag{2.8}$$

$$\left(h^a-i\frac{\partial}{\partial t}\right)\psi^a=0. \tag{2.9}$$

In this approximation, the two-electron wave functions ϕ^{ne}_j are written as antisymmetrized products of a core orbital χ^c and a diabatic orbital, $\chi^a_{1,2}$, for the active electron. The ensuing relationship between two- and single-electron approaches is cumbersome, except in the case in which active and core orbitals are orthogonal, and the electron-electron repulsion integrals between core and active electrons can be neglected. Then, the two-electron matrix elements are identical to the one-electron matrix elements for the active electron:

$$\langle \phi_i^{ne}|H|\phi_j^{ne}\rangle \simeq \langle \chi_i^a|h^a|\chi_j^a\rangle,$$
$$\langle \phi_i^{ne}|H|\phi_i^{ne}\rangle - \langle \phi_j^{ne}|H|\phi_j^{ne}\rangle \simeq \langle \chi_i^a|h^a|\chi_i^a\rangle - \langle \chi_j^a|h^a|\chi_j^a\rangle, \tag{2.10}$$

and, in this limit, the nonequivalent formalism reduces to the monoelectronic model of Eq. (2.9). Examples of applications can be found in ion -H^- collisions [16,17].

B. Use of the Landau-Zener-Stueckelberg and Landau-Zener models for the single-electron case

As mentioned in the Introduction, we shall study the validity of the different approaches by assuming that the LZS model is sufficiently exact in the solution of Eqs. (2.4) or (2.9). We assume that the molecular orbitals $\chi_{1,2}$ or $\chi_{1,2}^a$ have energies that cross, and we use the linear model for this crossing. For example, taking the explicit case of the equivalent electron model,

$$h_{22}-h_{11}=a(R-R_0),$$
$$h_{12}=c, \tag{2.11}$$

where R_0 is the crossing distance and c and a are constants. The solution of Eq. (2.4) is then expressed as

$$\psi(\mathbf{r},t)=a_1(t)\chi_1+a_2(t)\chi_2. \tag{2.12}$$

In order to simplify the formalism, we introduce the parameters

$$\alpha=\frac{R_0^2c^2}{v^2},$$
$$\beta=\frac{R_0^2a}{v}, \tag{2.13}$$

and we employ scaled distances $\overline{Z}=Z/R_0$, $\overline{b}=b/R_0$. Substitution of ψ in Eq. (2.4) and use of Eqs. (2.11), and (2.13) lead to the system of differential equations:

$$i\frac{da_1}{d\overline{Z}}=\sqrt{\alpha}a_2-(\beta/2)[\sqrt{\overline{b}^2+\overline{Z}^2}-1]a_1,$$
$$i\frac{da_2}{d\overline{Z}}=\sqrt{\alpha}a_1+(\beta/2)[\sqrt{\overline{b}^2+\overline{Z}^2}-1]a_2, \tag{2.14}$$

where

$$\overline{Z}=\frac{vt}{R_0}=\frac{\sqrt{R^2-b^2}}{R_0} \tag{2.15}$$

and $\langle \chi_i|\partial/\partial\overline{Z}|\chi_j\rangle=0$. If the collisional system is initially described by the orbital χ_1, the transition probability to χ_2 is given by

$$P^{\mathrm{LZS}}(\alpha,\beta,\overline{b})=|a_2(+\infty)|^2 \tag{2.16}$$

and the total capture cross section, in units of R_0^2, is

$$\sigma^{\mathrm{LZS}}(\alpha,\beta)=2\pi\int_0^\infty \overline{b}P^{\mathrm{LZS}}(\alpha,\beta,\overline{b})d\overline{b}. \tag{2.17}$$

The simple Landau-Zener (LZ) model is obtained by introducing the additional approximation that transitions take place only at $R=R_0$, and phase effects are neglected. The transition probability at $R=R_0$ is

$$p=1-q=1-\exp\left[-\frac{2\pi\alpha}{\beta\sqrt{1-\overline{b}^2}}\right]. \tag{2.18}$$

For collisions with $b>R_0$, the crossing is not traversed during the trajectory and no transitions take place, while for $b<R_0$ the crossing is traversed twice, at $\overline{Z}_\pm=\pm\sqrt{1-\overline{b}}$. After the crossing is traversed once, ($\overline{Z}_-<\overline{Z}<\overline{Z}+$), the populations of the diabatic states χ_1,χ_2 are, respectively, $1-p=q$ and $p=1-q$. Alternatively, one can employ the adiabatic orbital representation, $\{\varphi_1,\varphi_2\}$, obtained by diagonalizing the Hamiltonian matrix (2.11), with $\varphi_1=\chi_1;\varphi_2=\chi_2$ at $R>>R_0$. Application of the LZ model leads to populations of $p(=1-q)$ and $1-p(=q)$ for φ_1 and φ_2 respectively, for $\overline{Z}_-<\overline{Z}<\overline{Z}+$. For $\overline{Z}>\overline{Z}_+$, the crossing is traversed twice and, neglecting interferences, the population of the function χ_2 ($\equiv\varphi_2$) is

$$P^{\mathrm{LZ}}\left(\frac{\alpha}{\beta},\overline{b}\right)=2p(1-p)=2q(1-q) \tag{2.19}$$

and the corresponding total cross section is only a function of α/β:

$$\sigma^{\mathrm{LZ}}\left(\frac{\alpha}{\beta}\right)=2\pi\int_0^1 \overline{b}P^{\mathrm{LZ}}\left(\frac{\alpha}{\beta},\overline{b}\right)d\overline{b}. \tag{2.20}$$

Finally, the perturbative limit ($p\ll 1$) of Eq. (2.20) is

$$\sigma_p^{\mathrm{LZ}}\left(\frac{\alpha}{\beta}\right)=8\pi^2\frac{\alpha}{\beta}. \tag{2.21}$$

III. PERFORMANCE OF THE IPM USING LZ PROBABILITIES

In the LZ approximation, the single-electron transition probabilities are given by Eqs. (2.18) and (2.19) (see also Table I). Use of the standard IPM leads, for one passage through the crossing region, and in the diabatic representation, to

$$p_e=(1-p)^2=q^2,$$
$$p_s=2p(1-p)=2q(1-q), \tag{3.1}$$
$$p_d=p^2=(1-q)^2,$$

where p_e is the probability of the two electrons to remain in the initial orbital χ_1, p_s is the probability to transfer one electron to χ_2, and p_d is the probability to transfer both electrons to χ_2. Similar relations for the adiabatic represen-

TABLE I. Populations of elastic and single-electron transfer channels after one and two passages through the crossing region as functions of the LZ one-electron transition probabilities [see Eq. (2.18)] q (first line) and p (second line).

Elastic	Monoelectronic	IPM	Hamre *et al.* [30]	Bielectronic
One crossing (diabatic)	q	q^2	q^2	q^2
	$1-p$	$(1-p)^2$	$(1-p)^2$	$(1-p)^2$
One crossing (adiabatic)	$1-q$	$(1-q)^2$	$1-2q+q^2$	$1-q^2$
	p	p^2	p^2	$2p-p^2$
Two crossings	$1-2q+2q^2$	$1-4q+8q^2-8q^3+4q^4$	$1-4q+8q^2-8q^3+4q^4$	$1-2q^2+2q^4$
	$1-2p+2p^2$	$1-4p+8p^2-8p^3+4p^4$	$1-4p+8p^2-8p^3+4p^4$	$1-4p+10p^2-8p^3+2p^4$
Single-electron transfer	**Monoelectronic**	**IPM**	**Hamre *et al.* [30]**	**Bielectronic**
One crossing (diabatic)	$1-q$	$2q(1-q)$	$1-q^2$	$1-q^2$
	p	$2p(1-p)$	$2p-p^2$	$2p-p^2$
One crossing (adiabatic)	q	$2q(1-q)$	$2q-q^2$	q^2
	$1-p$	$2p(1-p)$	$1-p^2$	$(1-p)^2$
Two crossings	$2q(1-q)$	$4q-12q^2+16q^3-8q^4$	$4q-8q^2+8q^3-4q^4$	$2q^2-2q^4$
	$2p(1-p)$	$4p-12p^2+16p^3-8p^4$	$4p-8p^2+8p^3-4p^4$	$4p-10p^2+8p^3-2p^4$

tation are given in Table I, as well as the corresponding transition probabilities when the crossing is traversed twice.

In order to analyze the behavior of the IPM probabilities, we consider the ''exact'' two-electron equation (2.1). We construct a two-electron basis [see Eq. (2.5)],

$$\phi_e = ||\chi_1\overline{\chi_1}||,$$
$$\phi_s = \frac{1}{\sqrt{2}}[||\chi_1\overline{\chi_2}|| + ||\chi_2\overline{\chi_1}||] \tag{3.2}$$

consisting of the collision entrance channel ϕ_e and the single-electron capture channel ϕ_s. Equation (2.6) reads

$$H_{es} \simeq \sqrt{2}h_{12},$$
$$H_{ss} - H_{ee} \simeq h_{22} - h_{11}. \tag{3.3}$$

Employing Eqs. (3.3), one finds that, when the energy curves of χ_1 and χ_2 cross at $R=R_0$, the energy curves of the two-electron states ϕ_e and ϕ_s also cross at the same point. A double electron capture state ϕ_d can also be defined as

$$\phi_d = ||\chi_2\overline{\chi_2}|| \tag{3.4}$$

and, using Eq. (2.6), one obtains

$$H_{dd} - H_{ss} \simeq h_{22} - h_{11} \tag{3.5}$$

so that the energy of the double electron transition state ϕ_d also crosses those of states ϕ_e and ϕ_s at $R=R_0$. The presence of this unphysical triple crossing reflects the intrinsic inadequacy of the IPM for double electron transitions at least in the low-velocity domain where a molecular approach is applicable, hence we shall exclude ϕ_d from the two-electron basis. This is meaningful for many systems for which two-electron transitions are negligible; this is, for example, the case of collisions of H^+ with atoms and molecules [27,30,31,38]. For the ensuing two-stated basis, we can employ the same analytical treatment of Eqs. (2.13)–(2.17) by substituting ψ by Ψ, $\{\chi_1,\chi_2\}$ by $\{\phi_e,\phi_s\}$, and, from Eq. (3.3), α by 2α. In particular, this leads to the LZ populations of the diabatic states $\{\phi_e,\phi_s\}$, by using Eqs. (2.18) and (2.19). These LZ populations (called bielectronic) are listed in Table I together with the IPM ones [Eq. (3.1)]. Diagonalization of the Hamiltonian matrix (3.3) in the ϕ_e,ϕ_s basis yields two adiabatic states, whose LZ populations during the collision are also listed in Table I. This table allows an explicit comparison of the IPM and two-electron probabilities, carried out in the frame of the LZ treatment. A similar comparison using LZS cannot be carried out analytically and is considered in the following section.

We have included in Table I the populations given by the method of Ref. [30]. We see that the expression for p_e using this method is identical to the corresponding one in the standard IPM, but p_s is given by the sum of the IPM values for p_s and p_d of Eq. (3.1). Furthermore, we have also included in Table I the one-electron transition probabilities (labeled monoelectronic), which, as shown in Sec. II, can be taken as corresponding to the nonequivalent independent electron treatment.

An additional illustration is given in Fig. 1, where we have plotted the probabilities for single-electron transition

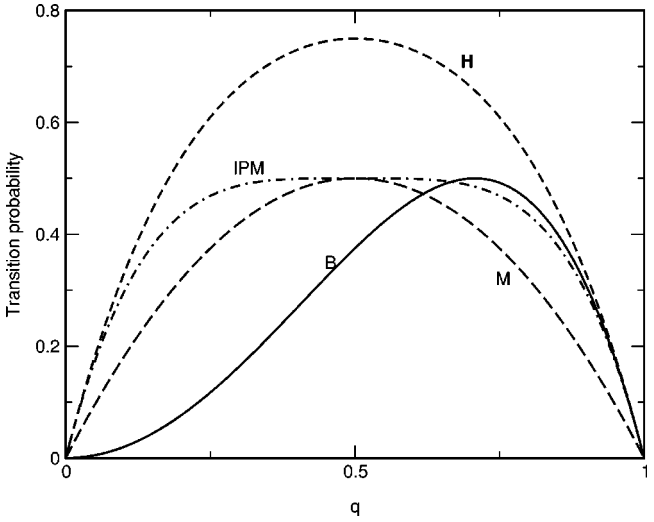

FIG. 1. Transition probabilities after two passages through the crossing point as functions of the one-electron transition probability q of Eq. (2.18): *M*, monoelectronic; *B*, bielectronic; IPM, standard IPM; *H*, modified IPM of Ref. [30].

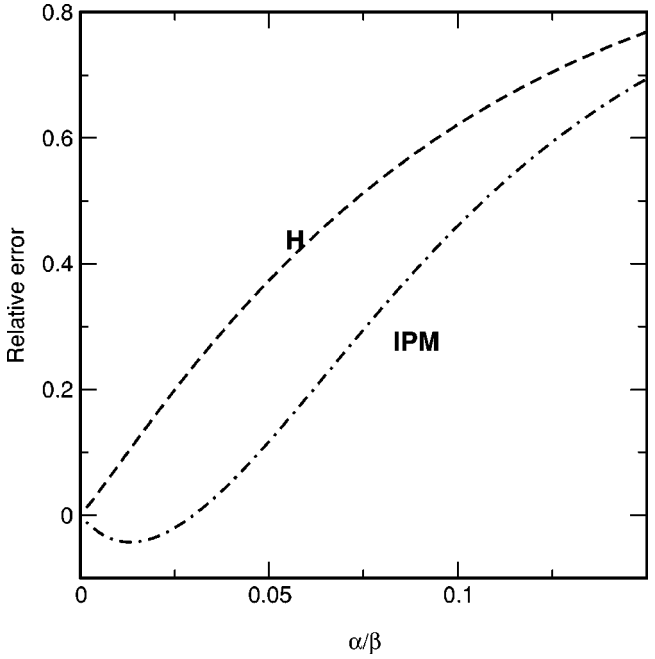

FIG. 2. Relative error $[(\sigma-\sigma^{\mathrm{bi}})/\sigma^{\mathrm{bi}}]$ in the LZ approximation, with σ calculated using the standard IPM (IPM) and the modified method of Ref. [30] (H).

after the collision as functions of the parameter q. Of course use of other parameters rather than q, such as α/β of Eq. (2.13), or q^2 would yield a different qualitative illustration of the results of Table I, for instance use of q results symmetrical monoelectronic probabilities and asymmetrical bielectronic results, whereas the opposite holds for q^2. From this figure and Table I, one can conclude the following in the frame of the LZ approximation.

(i) The IPM provides a good approximation to the bielectronic values in a wide range of physical situations with $q>0.6$, the differences being smaller than 10%. When $q\rightarrow 1$, the IPM and bielectronic results converge and correspond to situations in which the crossing is traversed diabatically and the perturbative expression (2.21) holds.

(ii) Table I explains the reasons for the good behavior of the IPM in the $p\ll 1$ limit. For instance, in the diabatic representation, the IPM reproduces exactly the population of the entrance channel in the way of the collision, thus indicating that the agreement in Fig. 1 is not fortuitous.

(iii) There appear important differences between nonequivalent (monoelectronic) and equivalent (IPM and bielectronic) probabilities of Fig. 1 for the whole range of values of q, with the exceptions $q=0$ (but not $q\rightarrow 0$), $q=0.5$, and $q\rightarrow 1$.

(iv) The modified IPM of Ref. [30] reproduces exactly the bielectronic result in the first part of the collision (see Table I). However, it overestimates the final single-electron transition probabilities; this overestimate is due to the fact that the unphysical value of p_d of the standard IPM is added completely to the single-electron transition probability. Hence, we conclude that in the present model application, the method of Ref. [30] offers no clear improvement over the usual IPM.

IV. CALCULATIONS

Our first calculation refers to the comparison of cross sections using the LZ model. Since the parameters p or q are not directly related to the Hamiltonian matrix elements [see, e.g., Eqs. (2.18) and (2.19)], we have evaluated the cross sections for single-electron transitions, in terms of the more meaningful scaled quantities α and β by integrating bielectronic and IPM transition probabilities of Table I. Furthermore, we have plotted in Fig. 2 the relative error of this cross section as a function of the parameter $\alpha/\beta=c^2/2\pi a v$ [see Eq. (2.20)]. This allows us to select the minimum velocity to apply the IPM with a given error for a particular crossing. As expected, the method of Ref. [30] leads always to larger deviations with respect to the bielectronic result than the standard calculation.

Next, we extend our analysis to the more exact LZS method. In this respect, we first compare in Fig. 3 the IPM and bielectronic cross sections obtained in the LZ and LZS models. It can be observed that, except for large values of α/β (>0.07) (see also Fig. 2), both approximations yield similar cross sections. It can be noted that the region $\alpha/\beta<0.07$ corresponds to values of the transition probability $q>0.6$ where the IPM and bielectronic probabilities agree (see Fig. 1). Complementary information is provided by the absolute errors $[(\sigma^{\mathrm{bi}}-\sigma^{\mathrm{IPM}})/\sigma^{\mathrm{IPM}}]$ plotted in Fig. 4, obtained by subtracting the corresponding cross sections plotted in Fig. 3.

Although the previous results are very encouraging with regards to the applicability of the IPM, the comparison in terms of the LZ model suffers from a drawback, in that both IPM and LZ approaches have a common limitation: from Eqs. (2.19) and (3.1) we see that they cannot provide transition probabilities larger than 0.5. Thus, in the numerical calculation of Refs. [32] it was concluded that the largest deviations of the IPM with respect to the *ab initio* results appear when the *ab initio* transition probability p_s reaches

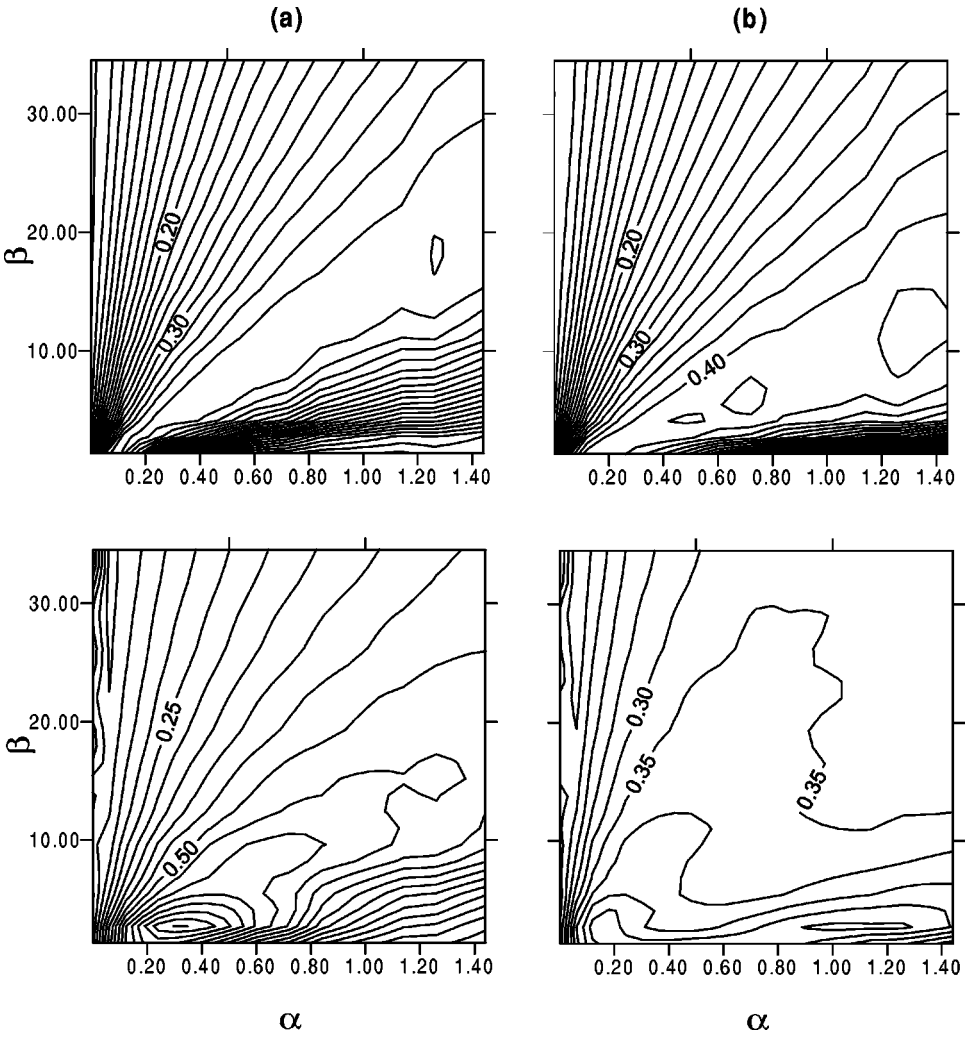

FIG. 3. Total cross sections for single-electron transition calculated with: (a) bielectronic transition probabilities; (b) IPM transition probabilities. Upper panels correspond to LZ and lower panels to LZS approaches.

values larger than 0.5, which cannot be obtained in the IPM calculation. Therefore, a comparison using the more exact LZS model is needed. In practice, this involves a solution of the system of differential equations (2.14) for given values of α and β to obtain $P^{\mathrm{LZS}}(\alpha,\beta,\overline{b})$ of Eq. (2.16). Use of the two-electron interpretation [see Eqs. (3.1)] leads to

$$P_s^{\mathrm{IPM}}(\alpha,\beta,\overline{b})=2P^{\mathrm{LZS}}(\alpha,\beta,\overline{b})[1-P^{\mathrm{LZS}}(\alpha,\beta,\overline{b})]. \tag{4.1}$$

For the same crossing, the bielectronic result is obtained as [see Eq. (3.3)]

$$P_s^{\mathrm{bi}}(\alpha,\beta,\overline{b})=P^{\mathrm{LZS}}(2\alpha,\beta,\overline{b}). \tag{4.2}$$

The transition probabilities P_s^{IPM} and P_s^{bi} have been integrated over the scaled impact parameter [see Eq. (2.17)] to obtain the corresponding total cross sections σ_s^{IPM} and σ_s^{bi}. In the illustration of Fig. 3, a noticeable decrease of σ_s^{IPM} can be observed with respect to σ_s^{bi} in the region in which the cross section is maximum. This is clearer from the absolute errors plotted in Fig. 4. The largest differences between the IPM and bielectronic cross sections appear in the region of values of α and β where the cross section is maximum and where the LZS results show noticeable differences from the LZ ones. An additional illustration of this point is provided by the transition probabilities plotted in Fig. 5. It can be noted that the IPM transition probabilities [Eq. (4.1)] reproduce the shape of the bielectronic transition probabilities when P_s^{bi} is smaller than 0.5, as in the case of Fig. 5(c), which indicates that the agreement in Fig. 4(b) is not fortuitous; however, the fact that Eq. (4.1) cannot yield transition probabilities greater than 0.5, leads to the distortion of the IPM curves with respect to the bielectronic ones in Figs. 5(a) and 5(b).

V. CONCLUSIONS

In this work, we have analyzed the usefulness of the widely applied IPM to calculate single-electron capture cross sections. We have considered a simple case that can be treated analytically, namely curve-crossing transitions in the Landau-Zener approximation, which furnishes the main mechanism of many dynamical problems. We have restricted our analysis to a situation of low electronic correlation, where the electronic Hamiltonian can be approximated as a sum of monolectronic Hamiltonians. This implies that the curve crossing between the two-electron energies arises from a crossing between the one-electron potential-energy curves

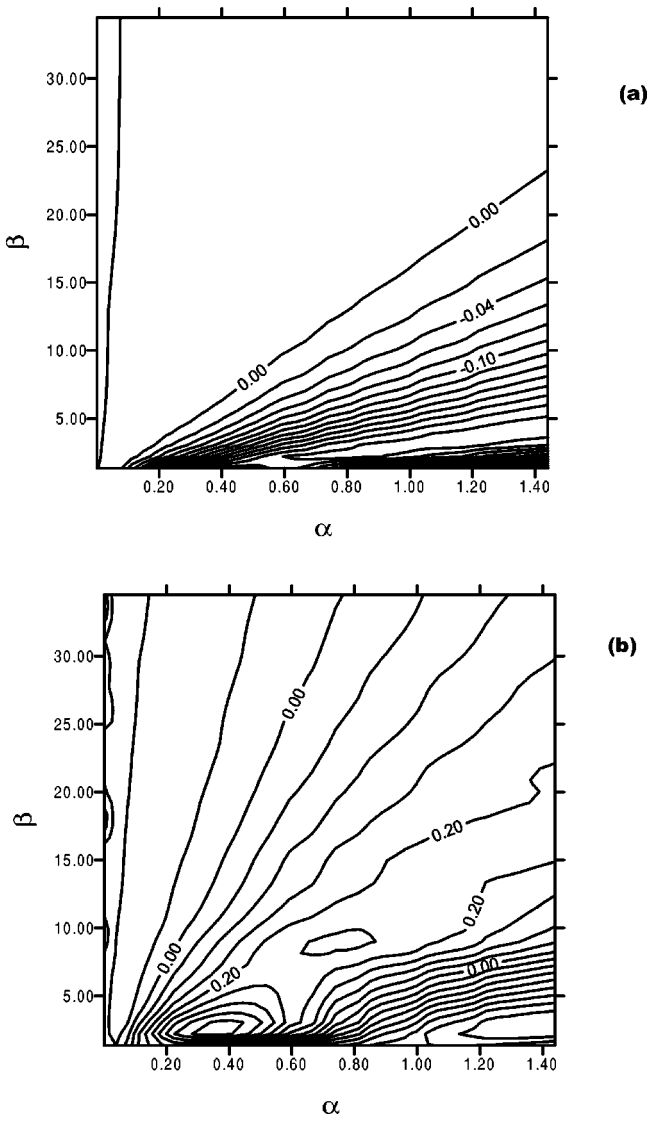

FIG. 4. Absolute errors ($\sigma^{\mathrm{bi}}-\sigma^{\mathrm{IPM}}$). (a) LZ model; (b) LZS model.

at the same internuclear distance, and there is a simple relationship between one- and two-electron Hamiltonian matrix elements (see Ref. [27]). Using the LZ approximation for the one- and two-electron cases, we have compared the populations of the two-electron states with those obtained in the IPM. We have shown that, in the diabatic representation, the IPM population of the entrance channel is exact for the first half of the collision. It further yields transition probabilities and cross sections for the whole collision in good agreement with the ''exact'' ones for many physical situations, and in particular at high impact velocities, where the diabatic representation is appropriate. This explains the success of the IPM at high energies.

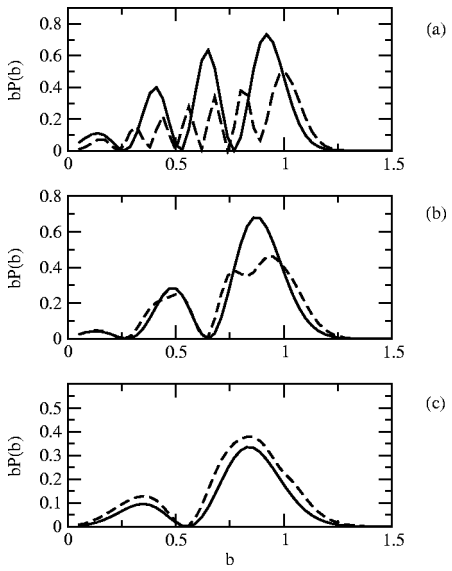

FIG. 5. Products of the scaled impact parameter $\bar{b}$ and the transition probabilities [see Eqs. (4.1) and (4.2)] $P_s^{\mathrm{bi}}(\alpha,\beta,\bar{b})$ (full line) and $P_s^{\mathrm{IPM}}(\alpha,\beta,\bar{b})$ (dashed line), as functions of $\bar{b}$. (a) $\alpha=1.4$, $\beta=20$; (b) $\alpha=0.62$, $\beta=13.3$; (c) $\alpha=0.35$, $\beta=10$. (These values of α and β correspond to constant values of a, c, R_0, and increasing velocity: (a) $v_0=R_0^2a/20$, (b) 1.5 v_0, (c) 2.0 v_0.)

The limitations of the IPM found in previous low-energy calculations [32] cannot be studied with the LZ model when the interference effects neglected in this model lead to transition probabilities greater than 0.5. To include these physical situations in our analysis, we have calculated numerically the transition probabilities by employing the LZS model. In particular, given a particular crossing, the contour plots of Fig. 4 can be used to estimate the error introduced by the IPM in the calculated cross section.

ACKNOWLEDGMENTS

This work has been partially supported by DGICYT Project Nos. BFM2000-0025 and FTN2000-0911.

[1] B. H. Bransden and M. H. C. McDowell, *Charge Exchange and the Theory of Ion-Atom Collisions* (Clarendon, Oxford, 1992).
[2] R. McWeeny, *Methods in Molecular Quantum Mechanics* (Academic Press, London, 1989).
[3] T. Kirchner, M. Horbatsch, H.J. Lüdde, and R.M. Dreizler, Phys. Rev. A **62**, 042704 (2000).
[4] R. Shingal and C.D. Lin, J. Phys. B **24**, 251 (1991).
[5] H.J. Lüdde, A. Macías, F. Martín, A. Riera, and J. Sanz, J. Phys. B **28**, 4101 (1995); T. Kirchner, L. Gulyás, H.J. Lüdde, E. Engel, and R.M. Dreizler, Phys. Rev. A **58**, 2063 (1998).
[6] R.E. Olson, J. Phys. B **12**, 1843 (1979); L. Meng, C.O. Reinhold, and R.E. Olson, Phys. Rev. A **40**, 3637 (1989).
[7] C. Illescas and A. Riera, Phys. Rev. A **60**, 4546 (1999).
[8] P.D. Fainstein, L. Gulyás, and A. Dubois, J. Phys. B **31**, L171 (1998).
[9] B. Zarour, J. Hansen, P.A. Hervieux, M.F. Politis, and F. Martín, J. Phys. B **33**, L707 (2000).

[10] I. Ben-Itzhak, A. Jain, and O.L. Weaver, J. Phys. B **26**, 1711 (1993).
[11] M.M. Sant'Anna, W.S. Melo, A.F. Santos, M.B. Shah, G.M. Sigaud, and E.C. Montenegro, J. Phys. B **33**, 353 (2000).
[12] A.M. Ermolaev, J. Phys. B **17**, 1069 (1984); R.J. Allan and J. Hansen, *ibid.* **18**, 1981 (1985); R. Shingal, B.H. Bransden, A.M. Ermolaev, D.R. Flower, C.W. Newby, and C.J. Noble, *ibid.* **19**, 309 (1986); R.J. Allan, *ibid.* **19**, 321 (1986); J.P. Salas, *ibid.* **33**, 3201 (2000).
[13] W. Fritsch and C.D. Lin, J. Phys. B **17**, 3271 (1984); M. Gargaud, R. McCarroll, and P. Valiron, *ibid.* **20**, 1555 (1987); B.C. Saha, Phys. Rev. A **51**, 5021 (1995); H.C. Tseng and C.D. Lin, *ibid.* **58**, 1966 (1998); L.F. Errea, J.D. Gorfinkiel, C. Harel, H. Jouin, A. Macías, L. Méndez, B. Pons, and A. Riera, J. Phys. B **32**, L673 (1999).
[14] R. Daniele, J. Chem. Phys. **72**, 1276 (1980); M. Gargaud, J. Hansen, R. McCarroll, and P. Valiron, J. Phys. B **14**, 2259 (1981); G. Peach, Comments At. Mol. Phys. **11**, 101 (1982); J. Pascale, Phys. Rev. A **28**, 632 (1983).
[15] O. Mó, A. Riera, and M. Yáñez, Phys. Rev. A **31**, 3977 (1985); L.F. Errea, L. Méndez, O. Mó, and A. Riera, J. Chem. Phys. **84**, 147 (1986); L. Méndez, I.L. Cooper, A.S. Dickinson, O. Mó and A. Riera, J. Phys. B **23**, 2797 (1990); L.F. Errea, B. Herrero, L. Méndez, O. Mó, and A. Riera, *ibid.* **24**, 4049 (1991); L. Féret and J. Pascale, Phys. Rev. A **58**, 3585 (1998); L. Fèret and J. Pascale, J. Phys. B **32**, 4175 (1999).
[16] A.M. Ermolaev, J. Phys. B **21**, 81 (1988); L. Errea, C. Harel, P. Jimeno, H. Jouin, L. Méndez, and A. Riera, *ibid.* **26**, 3573 (1993); L.F. Errea, C. Harel, P. Jimeno, H. Jouin, L. Méndez, and A. Riera, Phys. Rev. A **54**, 967 (1996); V. Sidis, C. Kubach, and D. Fussen, Phys. Rev. Lett. **47**, 1280 (1981); V. Sidis, C. Kubach, and D. Fussen, Phys. Rev. A **27**, 2431 (1983).
[17] A.M. Ermolaev and C.J. Joachain, Phys. Rev. A **62**, 012710 (2000).
[18] V.J. Montemayor and G. Schiwietz, J. Phys. B **22**, 2555 (1989); L. Meng, R.E. Olson, R. Dörner, J. Ullrich, and H. Schmidt-Böcking, *ibid.* **26**, 3387 (1993).
[19] J.H. McGuire and L. Weaver, Phys. Rev. A **16**, 41 (1977); V. Sidorovich, J. Phys. B **14**, 4805 (1981); H.J. Lüdde and R.M. Dreizler, *ibid.* **18**, 107 (1985).
[20] N.C. Deb and D.S.F. Crothers, J. Phys. B **23**, L799 (1990).
[21] Z. Chen, R. Shingal, and C.D. Lin, J. Phys. B **24**, 4215 (1991).
[22] H. Cederquist, E. Beebe, C. Biedermann, A. Engström, H. Gao, R. Hutton, J. Levin, L. Liljeby, T. Quinteros, N. Selberg, and P. Sigray, J. Phys. B **25**, L69 (1992).
[23] B. Bhattacharjee, M. Das, N.C. Deb, and S.C. Mukherjee, Phys. Rev. A **54**, 2973 (1996).
[24] R.K. Janev, E.A. Solov'ev, and D. Jakimovski, J. Phys. B **28**, L615 (1995).
[25] Y.D. Wang, C.D. Lin, N. Toshima, and Z. Chen, Phys. Rev. A **52**, 2852 (1995).
[26] A.L. Ford, L. Wehrman, K.A. Hall, and J.F. Reading, J. Phys. B **30**, 2889 (1997).
[27] D. Elizaga, L.F. Errea, J.D. Gorfinkiel, L. Méndez, A. Macías, A. Riera, A. Rojas, O.J. Kroneisen, T. Kirchner, H.J. Lüdde, A. Henne, and R.M. Dreizler, J. Phys. B **32**, 857 (1999).
[28] M. Gargaud and R. McCarroll, J. Phys. B **18**, 463 (1985).
[29] A. Kumar and B.C. Saha, Phys. Rev. A **59**, 1273 (1999).
[30] B. Hamre, J. Hansen, and L. Kocbach, J. Phys. B **32**, L127 (1999).
[31] T. Kirchner, H.J. Lüdde, M. Horbatsch,and R.M. Dreizler, Phys. Rev. A **61**, 052710 (2000).
[32] L. Errea, J.D. Gorfinkiel, C. Harel, H. Jouin, A. Macías, L. Méndez, B. Pons, and A. Riera, J. Phys. B **33**, 3107 (2000).
[33] M. McCartney, J. Phys. B **30**, L155 (1997).
[34] B.B. Dahl, L.C. Tribedi, U. Tiwari, P.N. Tandon, T.G. Lee, C.D. Lin, and L. Gulyás, J. Phys. B **33**, 1069 (2000).
[35] L.D. Landau, Phys. Z. Sowjetunion **2**, 46 (1932).
[36] C. Zener, Proc. R. Soc. London, Ser. A **137**, 696 (1932).
[37] E.C.G. Stueckelberg, Helv. Phys. Acta **5**, 369 (1932).
[38] D. Elizaga, L.F. Errea, J.D. Gorfinkiel, A. Macías, L. Méndez, A. Riera, and A. Rojas, J. Phys. B **33**, 2037 (2000).